Supplementary Information

Interfacial engineering with Carbon-Graphite-$Cu_\delta Ni_{1-\delta}O$ composites for ambient-air stable hole-conductor-free perovskite solar cells

Yousheng Wang*, Yuzhao Yang, Shaohang Wu, Cuiling Zhang, Zhen Wang, Jinlong Hu, Chong Liu, Fei Guo and Yaohua Mai*

Institute of New Energy Technology, College of Information Science and Technology, Jinan University, Guangzhou 510632, China

*E-mail address: wangys0120@jnu.edu.cn;

*E-mail address: yaohuamai@jnu.edu.cn;

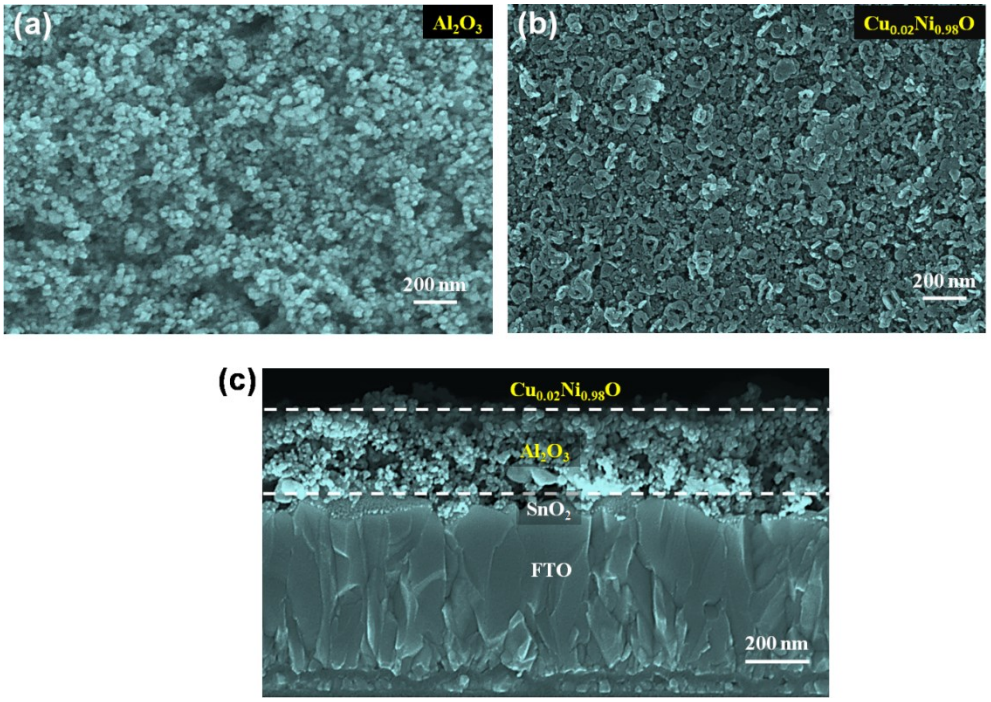

Figure S1 (a) The surface morphology of Al_2O_3 and (b) as-synthesized $Cu_{0.02}Ni_{0.98}O$ thin film and (c) cross-sectional SEM image of FTO/SnO_2/Al_2O_3/$Cu_{0.02}Ni_{0.98}O$.

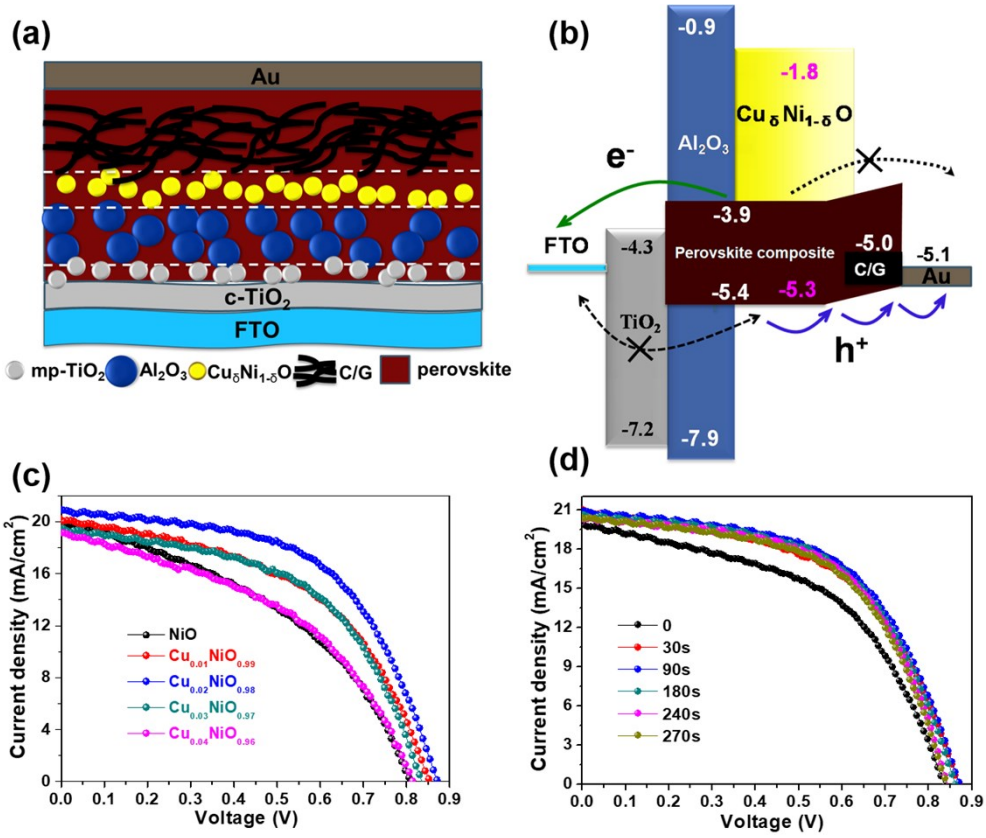

Figure S2 (a) Schematic of device configuration of FTO/c-TiO_2/mp-TiO_2/Al_2O_3/$Cu_\delta Ni_{1-\delta}O$/C-G/$MAPbI_{3-x}Cl_x$/Au and (b) corresponding the band energy diagram; (c) *J-V* performance for different Cu doping contents of $Cu_\delta Ni_{1-\delta}O$ films; (d) continuous 1-sun illumination effect of carbon based HCF device of $Cu_{0.02}Ni_{0.98}O$.

Table S1 Photovoltaic parameters (Figure S2c) of carbon based HCF-PSCs FTO/c-TiO_2/mp-TiO_2/Al_2O_3/$Cu_\delta Ni_{1-\delta}O$/C-G/$MAPbI_{3-x}Cl_x$/Au for different Cu doping contents of $Cu_\delta Ni_{1-\delta}O$ films.

δ ($Cu_\delta Ni_{1-\delta}O$)	V_{oc} (V)	J_{sc} (mA/cm^2)	FF (%)	PCE (%)
0	0.82	20.25	41.66	6.92
0.01	0.86	20.28	49.28	8.60
0.02	0.88	20.97	55.30	10.21
0.03	0.84	19.55	52.35	8.60
0.04	0.83	19.13	44.21	7.02

Table S2 Photovoltaic parameters (Figure S2d) for continuous 1-sun illumination effect of carbon based HCF device FTO/c-TiO_2/mp-TiO_2/Al_2O_3/$Cu_{0.02}Ni_{0.98}O$/C-G/$MAPbI_{3-x}Cl_x$/Au.

Photo-stability (s)	V_{oc} (V)	J_{sc} (mA/cm^2)	FF (%)	PCE (%)
0	0.84	19.81	49.94	8.32
30	0.88	20.95	52.87	9.75
90	0.88	20.97	55.30	10.21
180	0.87	20.62	55.41	9.95
240	0.85	20.26	56.67	9.76
270	0.85	20.30	55.85	9.64

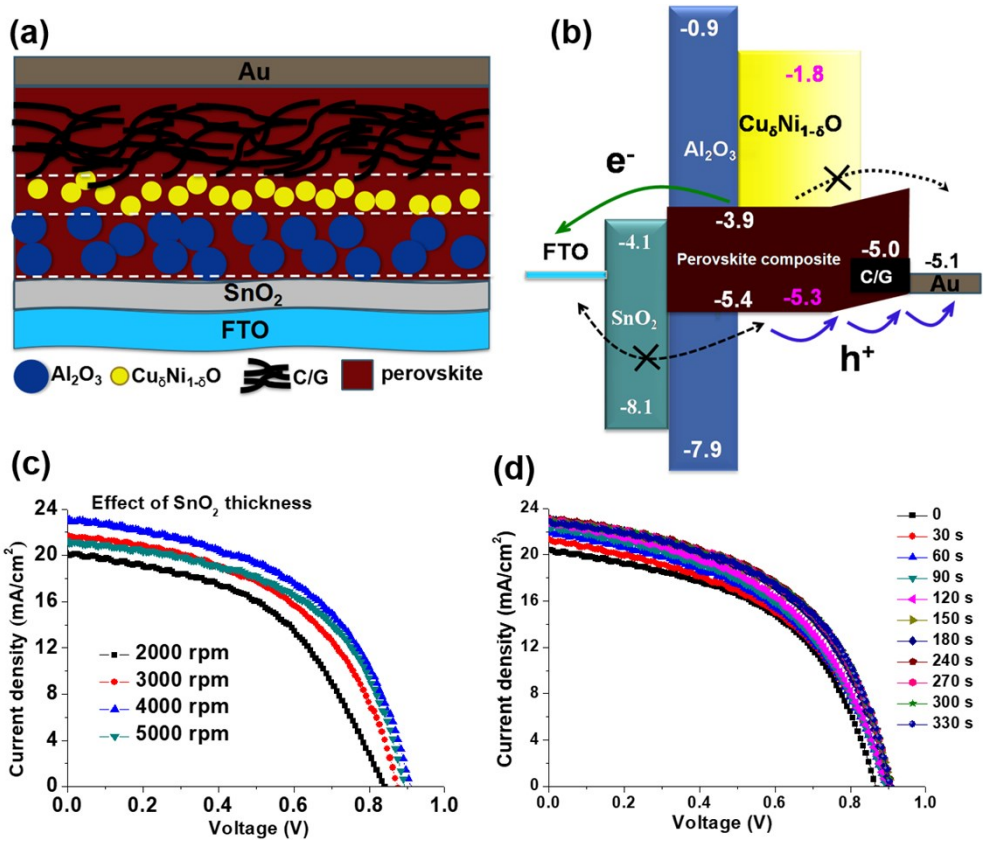

Figure S3 (a) Schematic of device configuration of FTO/SnO_2/Al_2O_3/$Cu_{0.02}Ni_{0.98}O$/C-G/$MAPbI_{3-x}Cl_x$/Au and (b) corresponding the band energy diagram; (c) corresponding *J-V* performance for different thicknesses of SnO_2 films; (d) continuous 1-sun illumination effect of Carbon and SnO_2 based HCF device for 4000 rpm of SnO_2.

Table S3 Photovoltaic parameters (Figure S3c) of carbon and SnO_2 based HCF-PSCs FTO/SnO_2/Al_2O_3/$Cu_{0.02}Ni_{0.98}O$/C-G/$MAPbI_{3-x}Cl_x$/Au for different rpm of SnO_2.

Spin-coating speed of SnO_2 precursor	V_{oc} (V)	J_{sc} (mA/cm^2)	FF (%)	PCE (%)
2000 rpm	0.84	20.01	47.64	8.01
3000 rpm	0.88	21.57	49.98	9.49
4000 rpm	0.91	23.01	52.12	10.92
5000 rpm	0.90	21.09	53.28	10.12

Table S4 Photovoltaic parameters (Figure S3d) for continuous 1-sun illumination effect of carbon and SnO_2 based HCF device of FTO/(4000 rpm) SnO_2/Al_2O_3/$Cu_{0.02}Ni_{0.98}O$/C-G/$MAPbI_{3-x}Cl_x$/Au.

Photo stability (s)	Voc (V)	Jsc (mA/cm^2)	FF (%)	PCE (%)
0	0.87	20.37	50.34	8.89
30	0.90	21.23	47.80	9.14
90	0.90	21.92	47.66	9.41
120	0.89	22.39	47.87	9.54
150	0.90	22.68	48.36	9.88
180	0.91	22.97	49.98	10.45
210	0.91	23.02	50.10	10.50
240	0.91	23.01	52.12	10.92
270	0.91	22.90	51.05	10.64
300	0.91	22.83	51.40	10.68
330	0.91	22.71	51.26	10.60

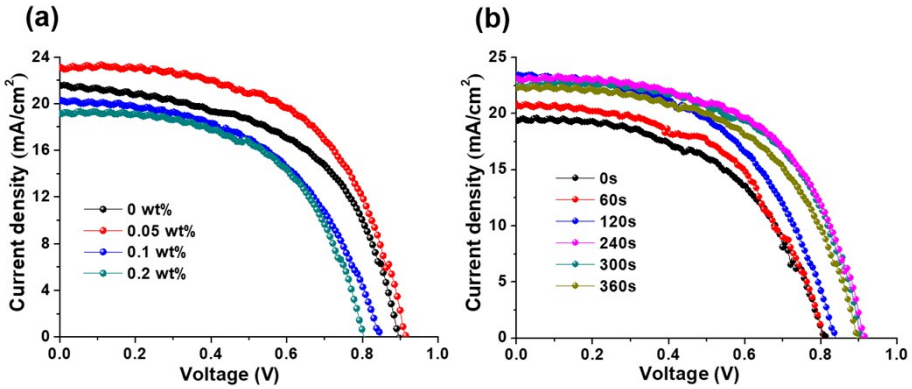

Figure S4 (a) *J-V* performance for different concentrations of $Cu_{0.02}Ni_{0.98}O$ NPs in C-G-$Cu_{0.02}Ni_{0.98}O$ composite films. (b) *J-V* performance for the continuous 1-sun illumination effect of C-G-$Cu_{0.02}Ni_{0.98}O$ composites and SnO_2 based HCF device of FTO/c-SnO_2/Al_2O_3/$Cu_{0.02}Ni_{0.98}O$/C-G-$Cu_{0.02}Ni_{0.98}O$-$MAPbI_{3-x}Cl_x$/Au.

Table S5 Photovoltaic parameters (Figure S4a) for different concentrations of $Cu_{0.02}Ni_{0.98}O$ NPs in C-G-$Cu_{0.02}Ni_{0.98}O$ composite based HCF-PSCs of FTO/SnO_2/Al_2O_3/$Cu_{0.02}Ni_{0.98}O$/C-G-$Cu_{0.02}Ni_{0.98}O$-$MAPbI_{3-x}Cl_x$/Au.

Contents of $Cu_{0.02}Ni_{0.98}O$	V_{oc} (V)	J_{sc} (mA/cm^2)	FF (%)	PCE (%)
w/o $Cu_{0.02}Ni_{0.98}O$	0.90	21.47	56.22	10.87
0.05 wt% $Cu_{0.02}Ni_{0.98}O$	0.92	22.97	56.23	11.88
0.1 wt% $Cu_{0.02}Ni_{0.98}O$	0.85	20.26	54.70	9.42
0.2 wt% $Cu_{0.02}Ni_{0.98}O$	0.81	19.13	52.13	8.07

Table S6 Photovoltaic parameters (Figure S4b) for continuous 1-sun illumination effect of 0.05 wt% $Cu_{0.02}Ni_{0.98}O$ NPs in C-G-$Cu_{\delta}Ni_{1-\delta}O$ composite based HCF device of FTO/SnO_2/Al_2O_3/$Cu_{0.02}Ni_{0.98}O$/C-G-$Cu_{0.02}Ni_{0.98}O$-$MAPbI_{3-x}Cl_x$/Au.

Photo stability (s)	V_{oc} (V)	J_{sc} (mA/cm^2)	FF (%)	PCE (%)
0	0.82	19.38	52.43	8.33
60	0.81	20.69	54.20	9.08
120	0.83	23.26	54.70	10.56
240	0.92	22.97	56.23	11.88
300	0.90	22.52	57.91	11.74
360	0.91	22.21	57.26	11.58

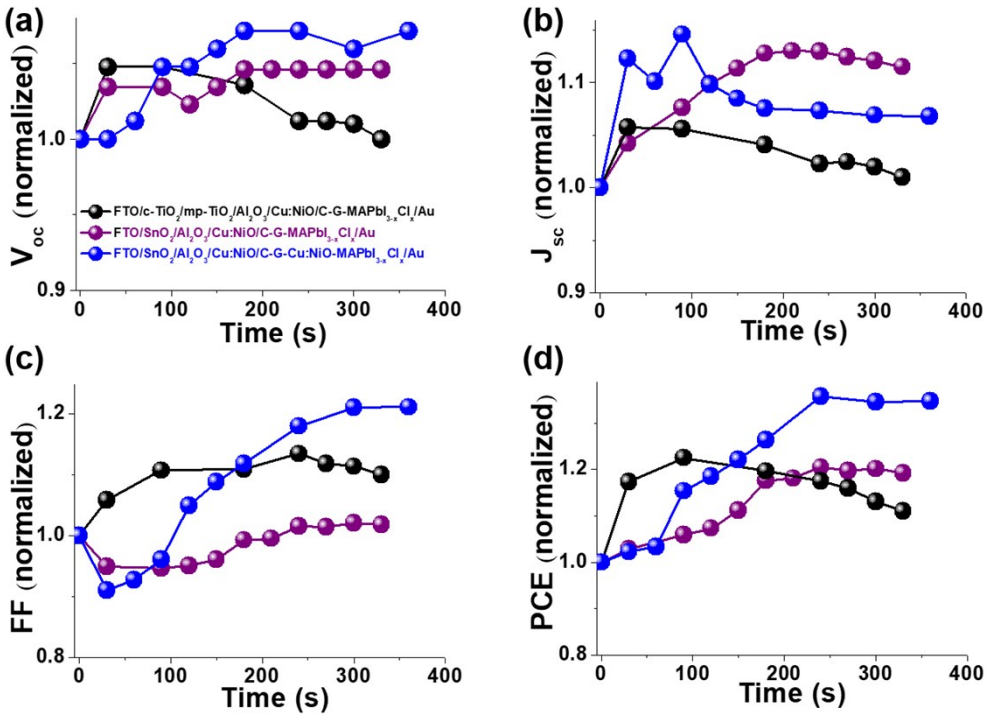

Figure S5 Light soaking effects of three types HCF devices under continuous 1-sun illumination: FTO/c-TiO_2/mp-TiO_2/Al_2O_3/$Cu_{0.02}Ni_{0.98}O$/C-G-$MAPbI_{3-x}Cl_x$/Au (black), FTO/SnO_2/Al_2O_3/$Cu_{0.02}Ni_{0.98}O$/C-G-$MAPbI_{3-x}Cl_x$/Au (purple) and FTO/SnO_2/Al_2O_3/$Cu_{0.02}Ni_{0.98}O$/C-G-$Cu_{0.02}Ni_{0.98}O$-$MAPbI_{3-x}Cl_x$/Au (blue).

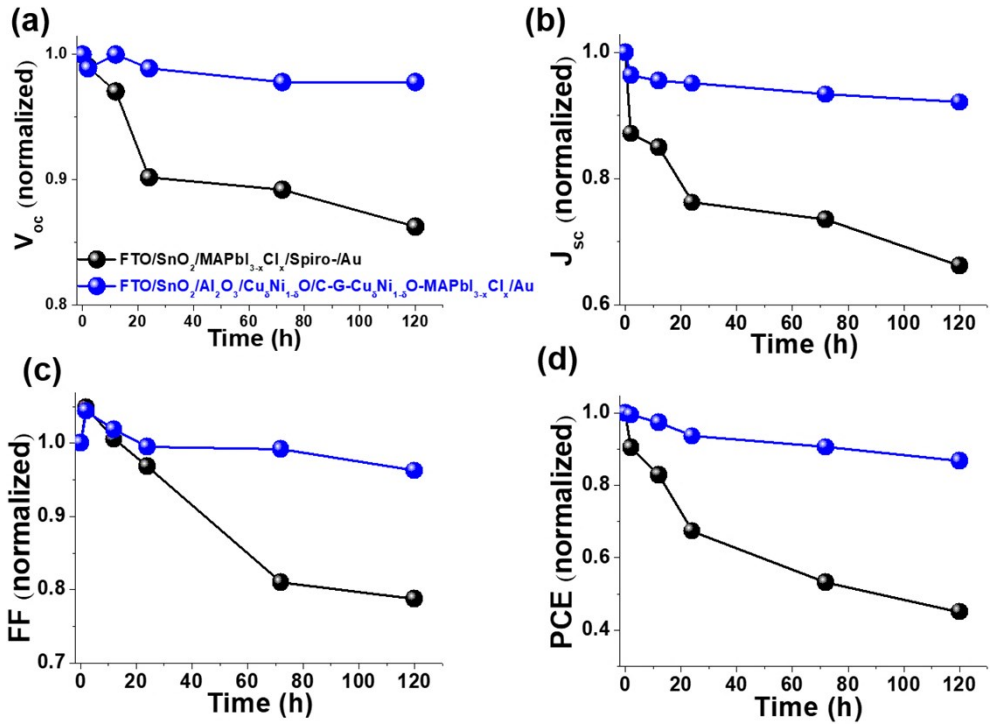

Figure S6 Thermal- and Air-stability for two devices of FTO/SnO_2/$MAPbI_{3-x}Cl_x$/Spiro-/Au (black) and FTO/SnO_2/Al_2O_3/$Cu_\delta Ni_{1-\delta}O$/C-G-$Cu_\delta Ni_{1-\delta}O$-$MAPbI_{3-x}Cl_x$/Au (blue) under 85 ℃ heat treatment and ambient air conditions (humidity 45-50%).

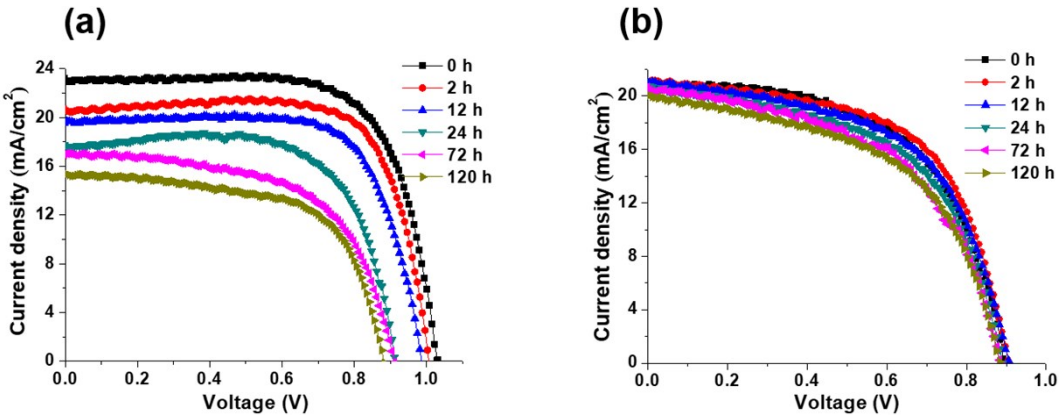

Figure S7 J-V (a) FTO/SnO_2/$MAPbI_{3-x}Cl_x$/Spiro-OMeTAD/Au, (b) FTO/SnO_2/Al_2O_3/$Cu_{0.02}Ni_{0.98}O$/C-G-$Cu_{0.02}Ni_{0.98}O$-$MAPbI_{3-x}Cl_x$/Au and corresponding *J-V* performance for thermal-stability at 85 ℃ in ambient air (45-50 % humidity).

Table S7 Photovoltaic parameters (Figure S6a) of FTO/SnO_2/$MAPbI_{3-x}Cl_x$/Spiro-OMeTAD/Au for thermal-stability at 85 ℃ in ambient air (45-50 % humidity).

Thermal stability (h)	V_{oc} (V)	Jsc (mA/cm^2)	FF (%)	PCE (%)
0	1.03	23.20	75.41	18.02
2	1.02	20.51	75.90	15.88
12	0.99	19.71	72.79	14.21
24	0.92	17.68	70.09	11.54
72	0.91	17.06	58.63	9.11
120	0.88	15.36	57.01	7.71

Table S8 Photovoltaic parameters (Figure S6b) of FTO/SnO_2/Al_2O_3/$Cu_{0.02}Ni_{0.98}O$/C-G-$Cu_{0.02}Ni_{0.98}O$-$MAPbI_{3-x}Cl_x$/Au for thermal-stability at 85 ℃ in ambient air (45-50 % humidity).

Thermal stability (h)	V_{oc} (V)	Jsc (mA/cm^2)	FF (%)	PCE (%)
0	0.91	21.97	56.23	11.24
2	0.90	21.17	58.68	11.18
12	0.91	20.98	57.27	10.94
24	0.90	20.89	55.94	10.52
72	0.89	20.51	55.77	10.18
120	0.89	20.34	55.72	10.09

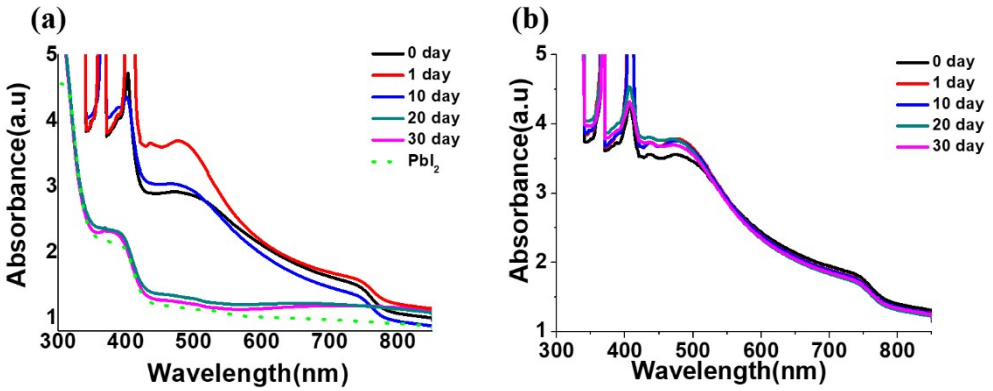

Figure S8 UV performance and thermal-stability for two films (a) FTO/SnO_2/$MAPbI_{3-x}Cl_x$/Spiro-OMeTAD, (b) FTO/SnO_2/Al_2O_3/$Cu_{0.02}Ni_{0.98}O$/C-G-$Cu_{0.02}Ni_{0.98}O$-$MAPbI_{3-x}Cl_x$ at 85 ℃ heating in ambient air (humidity 45-50 %).

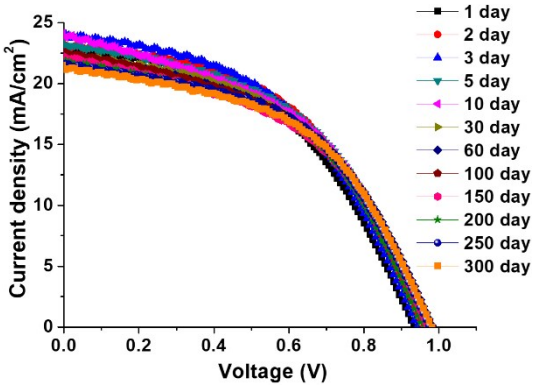

Figure S9 Schematic of device configurations FTO/SnO_2/Al_2O_3/$Cu_{0.02}Ni_{0.98}O$/C-G-$Cu_{0.02}Ni_{0.98}O$-$MAPbI_{3-x}Cl_x$/Au and corresponding *J-V* performance for long-term stability in ambient air (45-50 % humidity).

Table S9 Photovoltaic parameters (Figure S9) of FTO/SnO_2/Al_2O_3/$Cu_{0.02}Ni_{0.98}O$/C-G-$Cu_{0.02}Ni_{0.98}O$-$MAPbI_{3-x}Cl_x$/Au for long-term stability in ambient air (45-50 % humidity).

Long-term stability	Voc (V)	J_{sc} (mA/cm^2)	FF (%)	PCE (%)
1 day	0.951	22.97	55.41	12.11
2 day	0.965	23.88	61.23	14.11
3 day	0.962	24.08	58.10	13.46
5 day	0.966	23.16	57.24	12.81
10 day	0.964	23.83	54.48	12.52
30 day	0.965	22.34	57.20	12.33
60 day	0.961	22.01	57.53	12.12
100 day	0.963	22.58	55.70	12.12
150 day	0.965	22.12	56.37	12.03
200 day	0.951	21.91	56.44	11.76
250 day	0.962	21.66	56.40	11.75
300 day	0.951	21.18	56.62	11.40